HAL
open science

Synthesis of composite powders composed of silver and carbon nanotubes by liquid-phase reduction method

Maël Pontoreau, Benjamin Thomas, Emmanuel Le Guen, Christine Bourda, Nada Kraiem, Lisa Andrey, Jean-François Silvain

To cite this version:

Maël Pontoreau, Benjamin Thomas, Emmanuel Le Guen, Christine Bourda, Nada Kraiem, et al.. Synthesis of composite powders composed of silver and carbon nanotubes by liquid-phase reduction method. Nano-Structures & Nano-Objects, 2020, 24, 100622 (9 p.). 10.1016/j.nanoso.2020.100622 . hal-02998545

HAL Id: hal-02998545

https://hal.science/hal-02998545

Submitted on 10 Nov 2020

HAL is a multi-disciplinary open access archive for the deposit and dissemination of scientific research documents, whether they are published or not. The documents may come from teaching and research institutions in France or abroad, or from public or private research centers.

L'archive ouverte pluridisciplinaire **HAL**, est destinée au dépôt et à la diffusion de documents scientifiques de niveau recherche, publiés ou non, émanant des établissements d'enseignement et de recherche français ou étrangers, des laboratoires publics ou privés.

Synthesis of composite powders composed of silver and carbon nanotubes by liquid-phase reduction method

Maël PONTOREAU[a,b], Benjamin THOMAS[a], Emmanuel LE GUEN[b], Christine BOURDA[b], Nada KRAIEM[a,c], Lisa ANDREY[a], Jean-François SILVAIN[a,c]

[a] CNRS, Univ. Bordeaux, Bordeaux INP, ICMCB, UMR 5026, F-33608, Pessac, France

[b] METALOR Technologie SAS, F-28190, Courville-sur-Eure, FRANCE

[c] Department of Electrical and Computer Engineering, University of Nebraska-Lincoln, Lincoln, NE, 68588, USA

Abstract

A successful synthesis of composite powders composed of both silver (Ag) particles and multi walled carbon nanotubes (MWCNTs) by liquid-phase reduction methods is reported. Based on previous work on electroless deposition of Ag on MWCNTs and the mixing technique called “modified molecular level mixing”, the novel procedure strongly controls the amount of individualized MWCNTs in the Ag/MWCNTs composite powders with a mass fraction of MWCNTs between 0.1 wt.% and 3 wt.%.

The results show that temperature and the concentration of the reducing agent have a significant impact on the growth of the Ag particles while the MWCNTs concentration influences the nucleation rate of Ag particles during synthesis of Ag/MWCNTs composite powders. Thermogravimetric analysis of the powder synthesized also show a catalytic effect of Ag particles on the oxidation of MWCNTs.

Keywords

Silver, multi-walled carbon nanotubes, composite powder, liquid-phase reduction, growth, nucleation

* +33 6 89 12 36 40, Mael-Pontoreau@protonmail.com

Introduction

Due to their high mechanical, good thermal and electrical conductivity [1]–[5], carbon nanotubes (CNTs) have drawn more and more attention over the past three decades. Consisting of sets of concentric cylindrical graphite shells, multi-walled carbon nanotubes (MWCNTs) are the type of CNTs which is preferentially compared to more expensive single-walled carbon nanotubes (SWCNTs). Among other things, CNTs have been identified as a potential reinforcement for metal matrix composite materials (MMC). For instance, MMC with silver (Ag) matrix and CNTs reinforcement could have many applications such as contact materials in electronics [6], [7], as electrodes materials [8] or in photovoltaic cells [9].

Nevertheless, one of the key challenges in MMC processing is to disperse homogeneously the reinforcement within the metal matrix (Ag, Cu, Al,…) [10]. Indeed, CNTs are extremely entangled when received in powder form due to both physical (high aspect ratio of CNTs) and chemical entanglement (Van der Waals interaction between CNTs) [11]. Consequently, different methods have been set up to de-agglomerate CNTs prior to mixing with the metal matrix. The solution based processing is the main route used nowadays. It consists in the joint use of an ultrasonic treatment to de-agglomerate the CNTs and use of organic species (mostly surfactants) that adsorb on CNTs surface to prevent their re-agglomeration in solution. The adsorption of organics species on the surface of CNTs is known as non-covalent functionalization and tremendous efforts have already been devoted to optimizing the dispersion of CNTs in aqueous solution [12]–[20]. The dispersion of CNTs in the surfactant aqueous solution was the starting point of several methods to homogeneously disperse CNTs within a metal matrix.

The existing experimental procedures using CNTs suspensions can be divided into two categories. Firstly, dealing with powder metallurgy techniques, suspensions of CNTs are mixed with a microscopic metallic powder by simple magnetic stirring [21]–[26] or ball-milling [27]. Following these procedures, CNTs are expected to be adsorbed on the surface of the metallic powder. Even if some results seem to demonstrate that CNTs can be homogeneously dispersed on the surface of metallic powders, the distribution of CNTs throughout the volume of the consolidated MMC is inherently not homogenous. Actually, CNTs are only located at grain boundaries which lead to the presence of areas with a high concentration of CNTs in the densified materials [28], [29].

In order to obtain MMC in which CNTs are dispersed homogeneously throughout the volume, the synthesis of composite powders is a popular technique. This second available

route consists of growing metal particles on the surface of CNTs so that CNTs are not only located, after densification, on grain boundaries of the metallic powders. Concerning the case of Ag/CNTs composite materials, much effort has been devoted to the production of Ag/CNTs composite particles following chemical liquid-phase reduction methods; either by electroless deposition [30]–[37] or by others routes such as “modified molecular level mixing” [38]–[40]. The key factor for the success of these procedures is to prevent CNTs from agglomerating in solution prior to the deposition of Ag particles on the surface of CNTs. Concerning electroless deposition, the required sensitizing/activation steps are detrimental for the stability of CNTs suspensions. Consequently, following a typical electroless deposition procedure, the deposition of Ag particles can only occur on agglomerated CNTs [35]. Actually, according to the literature, researchers still struggle to obtain homogenous dispersion of CNTs within a Ag matrix by electroless deposition. Initially developed by Cha et al. [41], [42] for Cu/CNTs composite materials, the technique called “molecular level mixing” has been adapted by Pal et al. [39] for the production of Ag/CNTs composite materials. This method consists in mixing a stable CNTs suspension with a Ag salt and then adding a reducing agent to reduce Ag ions on the surface of CNTs. Consequently, applied to Ag, the “molecular level mixing” procedure is actually similar to the electroless deposition method without the sensitizing/activation step. The results are promising and the distribution of CNTs within the metal matrix seems to be improved. Nevertheless, that kind of procedure needs to be optimized as high concentrated zones of CNTs have been analyzed in the consolidated composite materials [43]. Moreover, the understanding of this mixing technique is partial since the mentioned studies do not give further details on the mechanisms involved in the synthesis of these composite powders.

Therefore, the aim of the present study is to bring essential information on the synthesis of Ag/CNTs composite powders by a chemical liquid-phase reduction method. The investigations presented range from the synthesis of pure Ag particles to heat treatment of Ag/MWCNTs composite powders. In addition, important modifications of the synthesis procedure presented in the literature are discussed in order to avoid the agglomeration of CNT. It should be remembered that the composite powders produced are intended to be densified to produce dense Ag/MWCNT composite materials which can be used as contact materials in electronics.

1. Experimental

1.1 Materials

For the synthesis of Ag/MWCNTs composite powders, MWCNTs were provided by US Research Nanomaterials® (fabricated by CCVD, purity 95 wt.%, length 10-30 μm, outside diameter 10-20 nm). Other chemical species involved are namely sodium dodecyl sulfate (SDS, Fisher Scientific®, purity 95%), silver nitrate ($AgNO_3$, Fisher Scientific®, purity 99%) and L-ascorbic acid (L-AA, $C_6H_8O_6$, Fisher Scientific, purity 99%). Ascorbic acid is a non-dangerous mild reducing agent (E = + 0.08 V) which has been chosen to reduce Ag ions (E = + 0.80 V) [44]–[46]. All solutions were prepared in 18 MΩ.cm-deionized water (known also as ultrapure water) for the synthesis of Ag/MWCNTs composite powder and distilled water was used subsequently to wash the synthesized powder.

1.2 Synthesis of composite powders

Firstly, MWCNTs were dispersed in an aqueous surfactant solution, as described in a previous work [12], to obtain dispersion of MWCNTs whose concentration is equal to 4.57 ± 0.16 g/L. Typically, for 1 L of a dispersion of MWCNTs, 1 g of MWCNTs was added in the aqueous surfactant solution in which 0.4 g of SDS was dissolved. The solution was sonicated 1 h with an ultrasonic homogenizer (Bandelin Sonopuls® UW2200) with active intervals of 0.1 s, passive intervals of 0.9 s, amplitude fixed at 50% and power equal to 200 W before being centrifuged for 5 min at 2680 g_0. Only the supernatant, was used for the synthesis of the composite powders. It is generally accepted that the suspensions obtained are composed of MWCNTs on the surface of which SDS molecules are adsorbed due to high hydrophobic forces.

Then, on the one hand, 15.8 g of $AgNO_3$ was dissolved in 500 mL of an aqueous solution. On the other hand, precise volume the MWCNTs dispersion was added in an aqueous solution containing L-AA to form a 500 mL solution. The added volume of the MWCNTs dispersion depends on the desired volume fraction of MWCNTs in the composite powder. It is important to point out that preliminary experiments show no agglomeration of MWCNTs even 3 days after mixing. Agglomeration of MWCNTs occurs if MWCNTs are mixed with $AgNO_3$ due to a significant increase in the ionic strength of the solution, which raises questions about procedures reported elsewhere [39], [40]. Unlike $AgNO_3$, the presence of L-AA do not increase sufficiently the ionic strength of the solution to induce agglomeration

of MWCNTs. Depending on the excess of L-AA used to reduce silver ions, the mass of dissolved L-AA equal to 8.2 g (L-AA1) or 32.7 g (L-AA4).

Separately, the two solutions were either heated to 70 °C or maintained at 5 °C via different water baths. Then, $AgNO_3$ solution was quickly poured into the solution containing the reducing agent and the MWCNTs under magnetic stirring (350 rpm). The instant color change of the solution confirmed the synthesis of Ag powder and that the following chemical reaction occurred:

$$2\ AgNO_3 + C_6H_8O_6 \rightarrow 2\ Ag\downarrow + C_6H_6O_6 + 2\ HNO_3 \qquad \text{Equation 1}$$

The solution was kept for 5 minutes under magnetic stirring before the resulting Ag/MWCNTs composite powder was separated from the solution by filtration. The composite powder was then washed several times with hot distilled water, then with ethanol and finally dried at 60 °C overnight. For each experiment carried out, around 10 g of powder were retrieved.

1.3 Investigation methods

The crystalline phases of the composite powders were analyzed by X-Ray diffraction (XRD) using a PANalitycal X'pert PRO MPD diffractometer with a Cu Kα radiation source (λ = 1.5406 Å).

Scanning electron microscopy (SEM) was performed to analyze the morphology and size of as produced Ag particles using a Tescan® Vega II microscope.

Analysis of the surface of as produced particles was carried out using a ThermoFischer Scientific K-Alpha® with a monochromatized Al Kα source ($h\nu$ = 1486.6 eV) and a 200 μm spot size. Full spectra and high resolution spectra obtained were fitted using the AVANTAGE software provided by ThermoFischer Scientific®. Scofield sensitivity factors were used for quantification.

Purity of Ag particles was assessed from thermogravimetric analysis (TGA) using a Setaram® TGA 24 thermal analyzer under ambient air or argon atmosphere with a heating rate of 5 °C/min. The mass fraction of MWCNTs in Ag/MWCNTs composite powders was determined by analyzing their carbon content using a C/S analyzer (ELTRA®, Carbon analyzer CS-2000).

2. Results and discussion

2.1 Preliminary study of reduction of pure Ag powder

Before synthetizing Ag/MWCNTs composite powders, pure Ag powders were obtained according to the experimental procedure described above except that the volume of the MWCNTs suspension added is zero. The reduction of Ag ions by L-AA has already been documented elsewhere [44]–[46]. Nevertheless, in the present work, the influence of the reduction temperature as well as the L-AA excess on the morphology of Ag particles is investigated into details. Figure 1 shows Ag particles synthesized at 5 °C or 70 °C and with an excess of L-AA equal to 1 or 4.

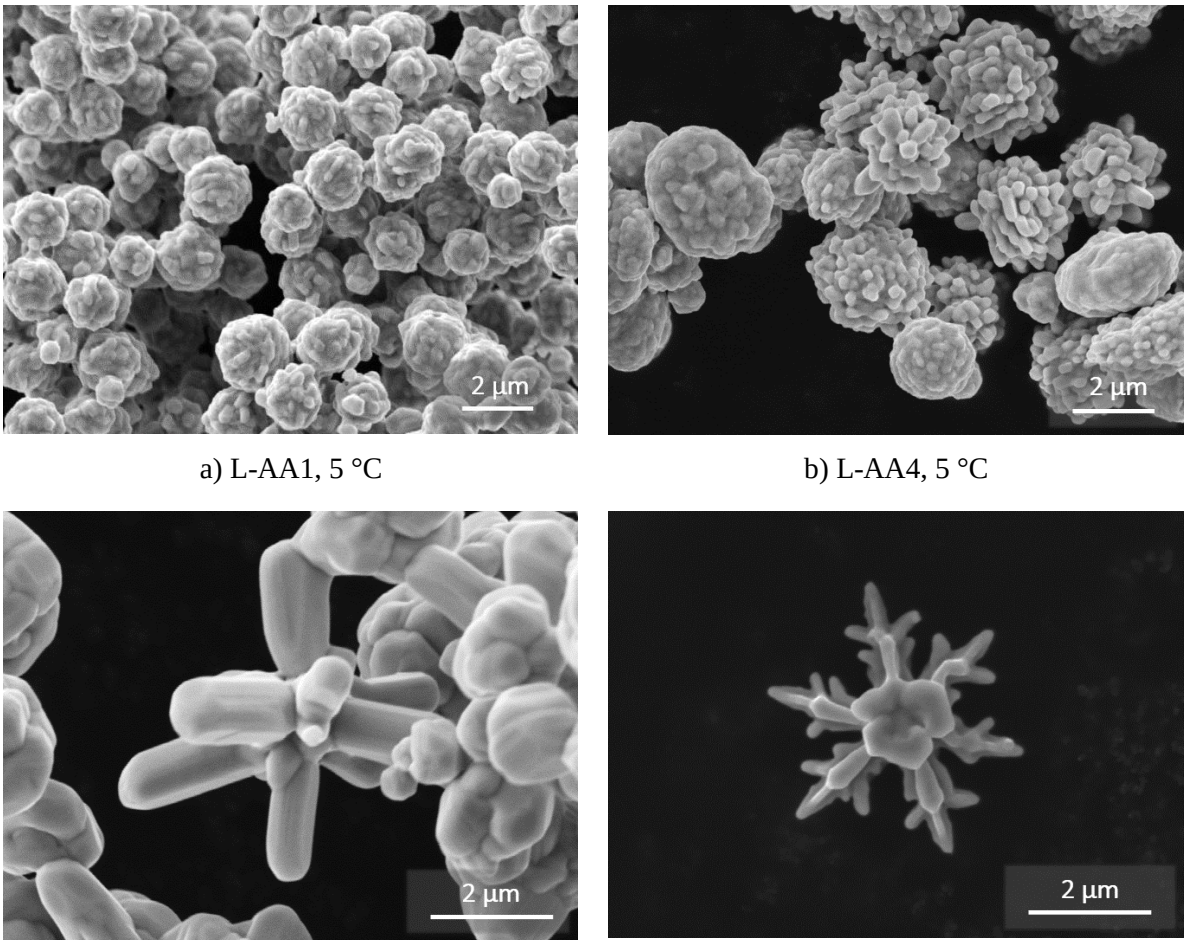

a) L-AA1, 5 °C b) L-AA4, 5 °C

c) L-AA1, 70 °C d) L-AA4, 70 °C

Figure 1 : SEM micrographs of pure Ag particles produced by chemical liquid-phase reduction with different L-AA excess and temperature

The Ag particles produced at 5 °C with L-AA excess equal to 1 are globally spherical (Figure 1 a). Analysis of the micrographs shows that the medium size of those spherical

particles is equal to 1.48 ± 0.21 μm. Increasing the L-AA excess from 1 to 4 (Figure 1 b), the size of Ag particles increases slightly. Most importantly, some significant protrusions appear at the surface of Ag particles. If the excess of L-AA is kept equal to 1 but the temperature is increased to 70 °C, the shape of Ag particles is irregular and some particles present consequential protrusions (Figure 1 c). Finally, using both a high excess of L-AA and temperature equal to 70 °C, Ag particles produced are mainly in the form of dendrites and some of them look like snowflakes (Figure 1 d).

Compared to spherical morphology, the hierarchical structures are not thermodynamically favored shape and are explained by kinetic factors. More particularly, formation of protrusions and then growth of dendrites are dependent on the concentration of the chemicals around the growth front, which is determined by the diffusion and reaction rates of chemicals [47]. By increasing the temperature and the excess of L-AA, the reaction rate is quickened to a point where the consumption of chemicals becomes faster than their supplement at the growth front. As a result, a chemical gradient is created around the growth front and the formation of loosely dendritic Ag structures is promoted as predicted by the Diffusion Limited Aggregation model [48]. Moreover, it has been proven that Ag dendrites grow along a preferential direction corresponding to <111> crystallographic directions [49], [50]. It seems that the reaction rate is more fasten by an increase of the temperature than an increase of L-AA excess. Indeed, protrusions are larger when only the temperature is increased than when only the L-AA excess is.

XRD patterns of the as-obtained Ag particles are shown in Figure 2. For the two XRD patterns, the diffraction peaks in the spectrum can be designated to (111), (200), (220), and (311) plans of Ag with a face centered cubic structure (JCPDS file No. 04-0783). Although the Ag particles have different morphologies, depending on the amount of AA and on the temperature, their crystal structures are similar in terms of relative peak intensity and width. No other crystalline faces have been detected, indicating Ag oxides or reaction residues are absent (at that analysis scale) from the Ag powder produced.

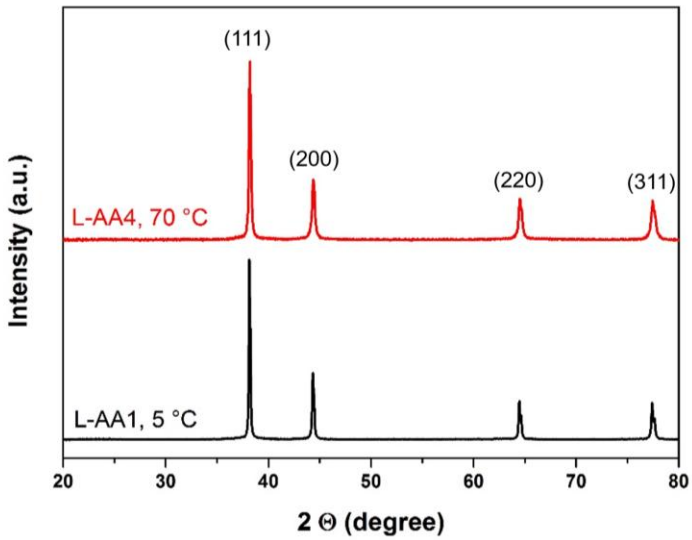

Figure 2 : XRD patterns of Ag particles synthesized at various temperature and various concentration of L-AA

To sum up, an increase of reaction temperature and, to a lesser extent, an increase of L-AA excess lead to an increase of the reaction rate, resulting in the switch of Ag particle morphologies from spheres to dendrites. More detailed work may be carried out to study further the reduction of Ag ions by AA.

2.2 Synthesis of Ag/MWCNTs composite powders

2.2.1 Nucleation and growth of composite powders

In this study, Ag/MWCNTs composite powders have been synthesized at 70 °C and with an excess of L-AA equal to 4. Figure 3 shows the morphology of the Ag/MWCNTs composite powders as a function of their mass percentage in MWCNTs.

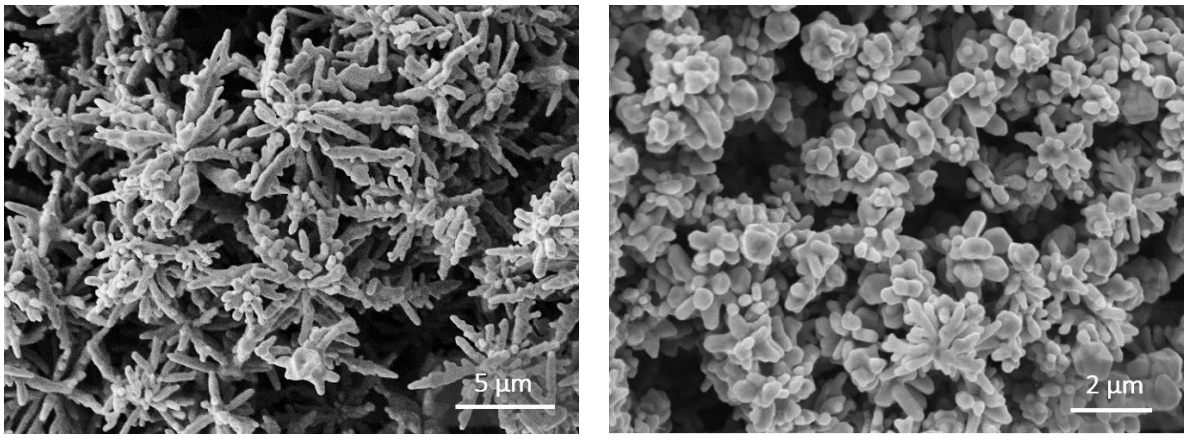

a) 0 wt.% b) 0.1 wt.%

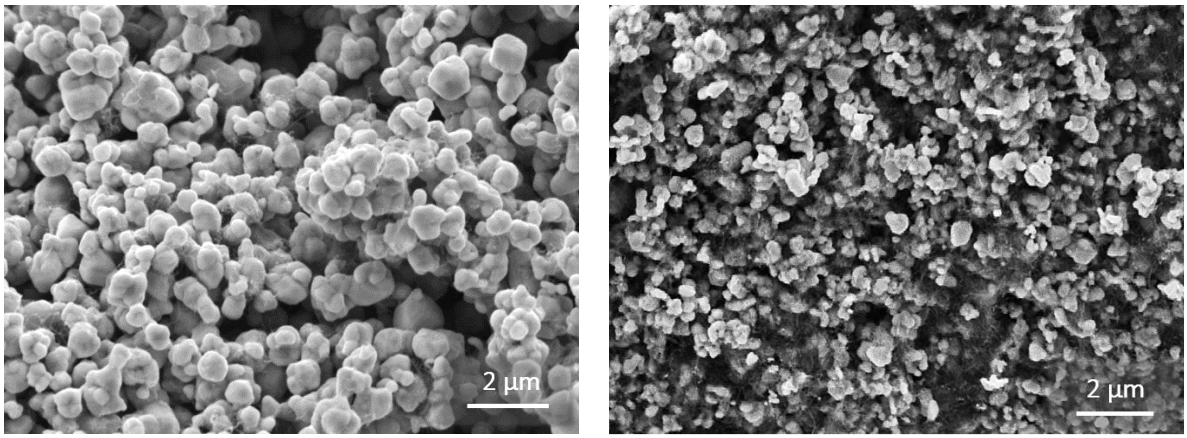

c) 0.4 wt.% d) 3 wt.%

Figure 3 : SEM micrographs of the Ag/MWCNTs composite powders produced by chemical liquid-phase reduction with different wt.% of MWCNTs

A general observation is that the morphology of Ag particles is significantly modified when the MWCNTs concentration increases. For the Ag/MWCNTs composite powders with 0.1 wt.% of MWCNTs (Figure 3 b), Ag particles still show “outgrowths” but their length is limited compared to pure Ag powder. With a further increase of the MWCNTs content to 0.4 wt.% (Figure 3 c), Ag particles are compact spheres and no “outgrowths” have been analyzed. Finally, for a further increase in MWCNTs content (Figure 3 d), the size of the compact Ag spheres decreases significantly. Indeed, the average diameter of Ag particles decreases from 0.76 ± 0.21 µm to 0.45 ± 0.22 µm for Ag/MWCNTs composite powders with a mass percentage of MWCNTs equal to 0.4 wt.% and 3 wt.% respectively.

To sum up, with the increase of the mass percentage of MWCNTs from 0 wt.% to 0.4 wt.% to 3 wt.% the morphology of the Ag particles changes from dendrites to microscopic compact spheres to submicron compact spheres, respectively. The modification of the morphology of the Ag particles can be explained in relation to the nucleation process. Without MWCNTs, Ag particles mainly arise from homogeneous nucleation as no impurities are present in the system. On the contrary, during the synthesis of composite powders, MWCNTs are present in suspension and induce heterogeneous nucleation of Ag particles on MWCNTs surface. Indeed, SDS molecules adsorbed on MWCNTs surface permit to counter the inherent chemical inertness of MWCNTs so that MWCNTs in suspension act as heterogeneous nucleation sites on the surface of which Ag particles nucleate and then grow, as discussed elsewhere [51]–[53]. An electrostatic attraction may exist between the anionic groups of sulfate in SDS molecules and with Ag^+ ions [53]. Therefore, the increase of the concentration

of MWCNTs induces an increase of heterogeneous nucleation sites and thus an increase of the global nucleation rate of Ag particles. In line with this idea, with a high nucleation rate, more Ag particles nucleate from the first moments of synthesis and thus the concentration of Ag ions in solution plunges. Consequently, the growth and the size of the Ag particles are lowered as the concentration of MWCNTs in solution increases. This assumption explains the modification of the morphology and the size of Ag particles for low MWCNTs concentration in suspension. Actually, the morphology of Ag particles is significantly impacted by a MWCNTs concentration equal to 0.01 g/L which corresponds to a MWCNTs mass percentage equal to 0.1 wt.%. Figure 4 illustrates the influence of MWCNTs on the synthesis of Ag particles by a chemical liquid-phase reduction in solution.

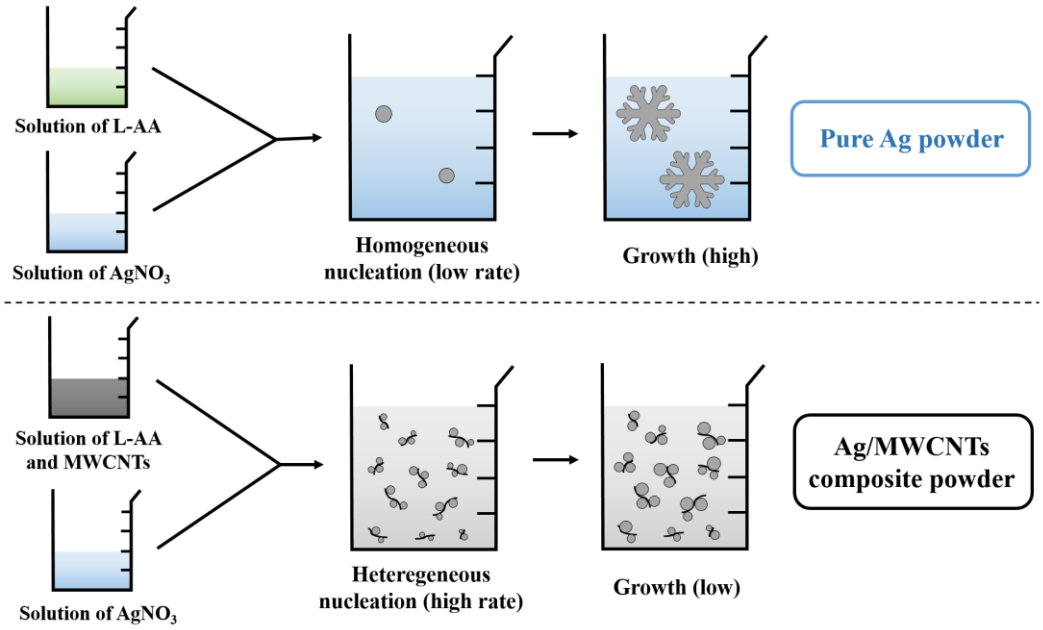

Figure 4 : Schematic of the reduction of Ag ions by chemical liquid-phase reduction with or without MWCNTs dispersed in solution (not at scale)

2.2.2 Distribution of MWCNTs within the Ag/MWCNTs composite powders

SEM analyses show that Ag is not deposited homogeneously around MWCNTs. Unlike electroless deposition, MWCNTs are not sensitized and activated so that MWCNTs are not covered with a large number of Pd particles acting as catalytic sites for the reduction of Ag ions in solution [35]. However, taking into account the desired mass fraction of MWCNTs, agglomeration of MWCNTs prior to Ag particle reduction would not result in

composite powders Ag/MWCNTs in which the MWCNTs are homogeneously dispersed. As discussed in the introduction, the absence of the sensitization and activation steps makes it possible to keep the MWCNTs individualized during the reduction of Ag particles and, thus to obtain composite powders in which MWCNTs are not agglomerated. Indeed, for composite powders with a mass percentage of MWCNTs below 0.8 wt.%, no MWCNTs agglomerates have been analyzed by SEM. Above 0.8 wt.%, few clusters of MWCNTs have been analyzed (Figure 5 a). Concerning the composite powders with 3 wt.% of MWCNTs, the amount of MWCNTs is too high so that MWCNTs percolate and form a network in which the Ag particles are distributed (Figure 5 b). Consequently, a threshold mass percentage of MWCNTs exists above which a network of MWCNTs is formed due to MWCNTs percolation. According to the experiment carried out, this threshold is estimated to be approximately around 0.8 wt.% for this specific type of MWCNTs.

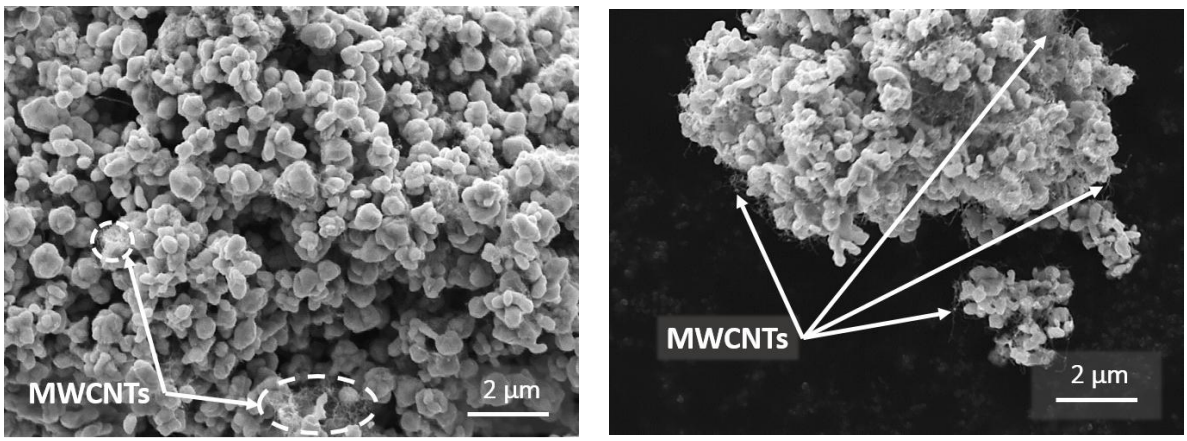

a) 0.8 wt.% b) 3 wt.%

Figure 5 : SEM micrographs of the Ag/MWCNTs composite powders produced by chemical liquid-phase reduction with different wt.% of MWCNTs

Therefore, even if the synthesis procedure do not permit to cover homogeneously the MWCNTs with Ag, the presented protocol lead to the synthesis of Ag/MWCNTs composite powder in which MWCNTs are individualized and homogeneously dispersed. For the intended applications (i.e. to produce dense Ag/MWCNTs composite materials), it is generally accepted that the volume fraction of MWCNTs in Ag/MWCNTs composite materials should not exceed 3 vol.% which is equivalent to a mass equal to 0.6 wt.%. Consequently, the distribution of MWCNTs within the Ag/MWCNTs composite powders is quite satisfactory in that range of composition. Above 0.6 wt.%, the composite powder begins to contain few NTC agglomerates which is not suitable for the intended application. In addition, it should be noted that Ag particles aggregate and form micro-sized aggregates after

the filtration, washing and drying steps. However, for the intended application, the formation of micro-sized aggregates is not detrimental. The advantages of this synthesis protocol will be discussed later in this article.

2.3 Heat treatment of Ag/MWCNTs composite powders

2.3.1 Highlighting of the surface pollution of Ag particles

The surface of pure Ag powder has been characterized by XPS. Figure 6 shows the survey spectrum of pure Ag powders (L-AA4, 70 °C) as well as high resolution spectra corresponding to Cl_{2p}, C_{1s}, Ag_{3d}, O_{1s}, Na_{1s} respectively. Although Ag powders have been carefully washed several times and no other crystalline phases have been analyzed by XRD, characterization of the surface of Ag particles indicates that some pollution is present on the surface of Ag particles. It is believed that the small amounts of chlorine and sodium atoms detected (around 2 at.%) come from the distilled water used to wash the powder. Indeed, for pure Ag particles, chlorine and sodium atoms come neither from the chemical species used ($AgNO_3$, L-AA) nor from the ultrapure water. Therefore, it is an unfortunate post-synthesis pollution located on the surface of Ag particles. Otherwise, quantification of the high resolution peaks shows that the amount of carbon and oxygen atoms is significantly high (around 35 at.% and 10 at.% respectively). Therefore, organic species must be adsorbed on the surface of the Ag particles coming from L-AA for pure Ag powder. This pollution must be present in the same way on the surface of Ag particles in Ag/MWCNTs composite powders. Even in small amounts, these organic pollutants on the surface of Ag particles may disrupt the sintering of these powders. Consequently, a heat treatment must be carried out prior sintering step in order to remove these organic compounds.

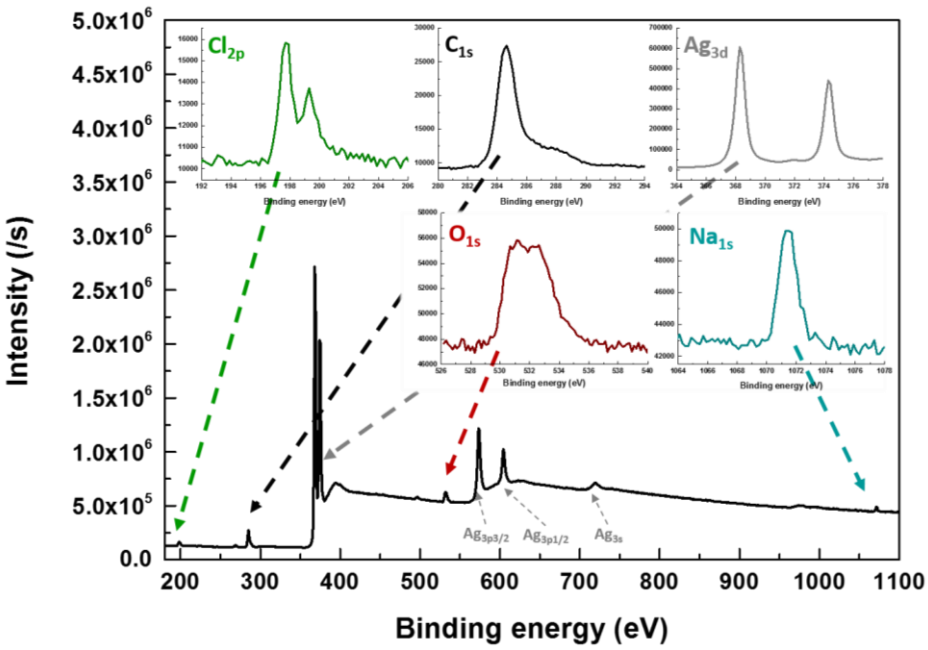

Figure 6 : XPS survey and high-resolution spectra of pure Ag particles

2.3.2 Thermal analysis of Ag/MWCNTs composite powders

Dealing with Ag/MWCNTs composite powders, the heat treatment must be set up in such a way that most of the pollution decomposes but not MWCNTs. Therefore, TGA of both pristine MWCNTs and a Ag/MWCNTs composite powder with 3 wt.% of MWCNTs have been performed over a temperature range of 50-750 °C with a heating rate of 5 °C/min under argon (Ar) gas and ambient air atmosphere (Figure 7 and Figure 8). Under ambient air, pristine MWCNTs are stable up to 450 °C and then are totally oxidized above 650 °C whereas the oxidation of MWCNTs, from Ag/MWCNTs composite powder, begins around 250 °C and finishes around 500 °C. Indeed, the mass loss of Ag/MWCNTs composite powder under ambient air is equal to 3% which corresponds perfectly to the predicted mass percentage of MWCNTs in the Ag/MWCNTs composite powder. According to the first derivate of these TGA curves, the kinetic of the thermal oxidation of MWCNTs reaches a maximum of around 600 °C and 350 °C for pristine MWCNTs and Ag/MWCNTs composite powder respectively. Due to oxygen partial pressure, oxidation of MWCNTs takes place according to the following reaction:

$$C(s) + O_2(g) \rightarrow CO_2(g) \qquad \text{Equation 2}$$

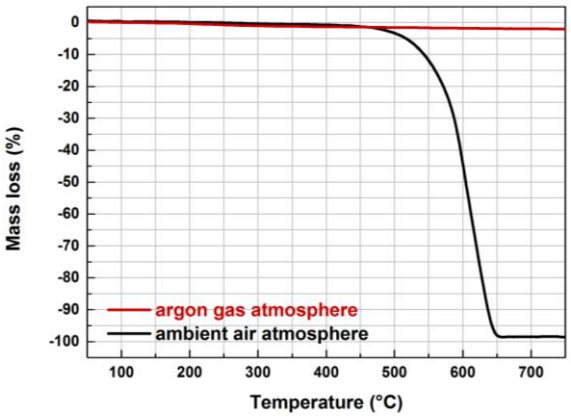

Figure 7 : TGA curve of pristine MWCNTs (5 °C/min)

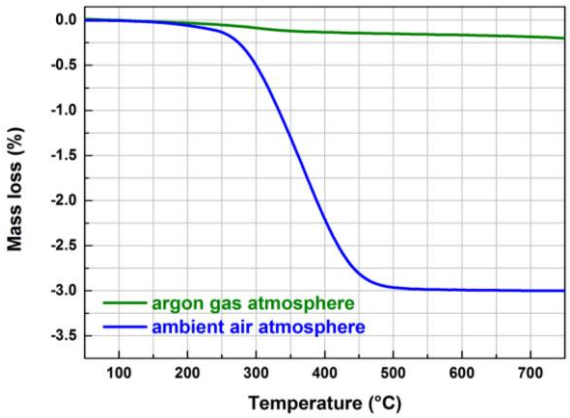

Figure 8 : TGA curve of Ag/MWCNTs composite powder with 3 wt.% of MWCNTs (5 °C/min)

The significant difference for the decomposition of MWCNTs can be explained by the role of Ag particles surrounding MWCNTs in the composite powder. Actually, Ag particles may act as catalyst particles which lower the temperature of calcination of MWCNTs, as also suggested by Aani *et al.* [54]. Nevertheless, under argon gas atmosphere, MWCNTs remain stable for both samples for the range of temperature studied. Under an Ar gas atmosphere, the oxygen partial pressure is so negligible that decomposition of MWCNTs does not take place.

Concerning the thermal decomposition of organic species present on the surface of Ag particles, TGA of L-AA and SDS have been performed under an Ar atmosphere (Figure 9 a). Major decomposition of these organic species occurs above 200 °C. The first derivative of the TGA curves (Figure 9 b) shows that the kinetic of thermal decomposition of these organic species reaches a maximum of around 220 °C. At 350 °C, the mass loss of L-AA and SDS is equal to 61 % and 74 % respectively. Therefore, the Ag/MWCNTs composite powders can be heat-treated under argon at 350 °C to remove most of the organic pollutants without oxidizing the MWCNTs.

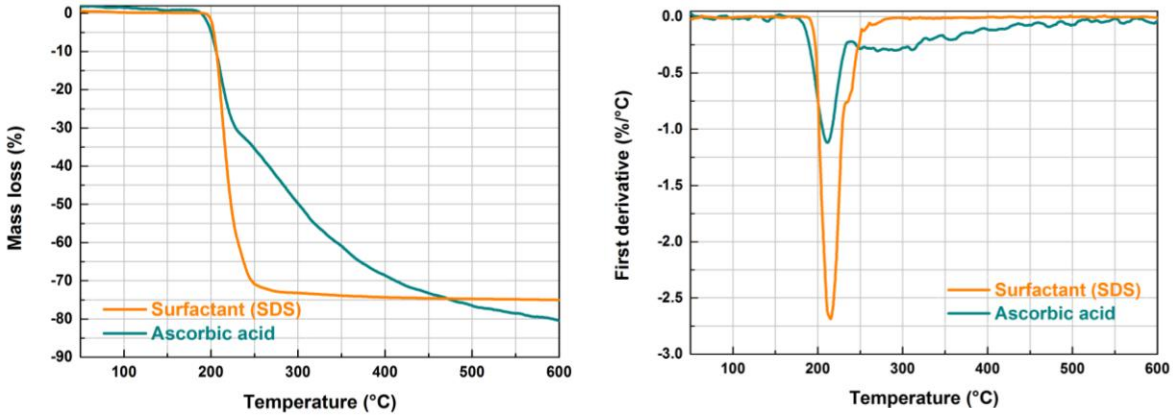

a) b)

Figure 9 : Thermal analysis (Ar, 5 °C/min) of the reducing agent (L-AA) and the surfactant (SDS) a) TGA curves b) and its first derivatives

2.3.3 Analysis of heat-treated Ag/MWCNTs composite powders

Synthesized Ag/MWCNTs composite powders have been heat-treated at 350 °C for one hour in a tubular furnace under constant Ar flow. Before and after the heat treatment, quantification of the carbon content of the Ag/MWCNTs composite powders has been performed. Figure 10 shows the analyzed carbon mass fraction of the different Ag/MWCNTs composite powder as a function of the theoretical MWCNTs mass fraction of the corresponding powder. Theoretical MWCNTs mass fraction ($x_{m,MWCNTs}$) is related to the volume of MWCNTs dispersion (V_{MWCNTs}) added before the reduction of Ag ions according to the following equation:

$$V_{MWCNTs} = (m_{Ag} * x_{m,MWCNTs})/(C_{MWCNTs} * (1 - x_{m,MWCNTs})) \qquad \text{Equation 3}$$

Theoretical computations take into account the uncertainties related to the different parameters, such as the uncertainty on the concentration of MWCNTs in suspension (C_{MWCNTs}) or the reduced mass of Ag (m_{Ag}). Absolute uncertainty is also plotted.

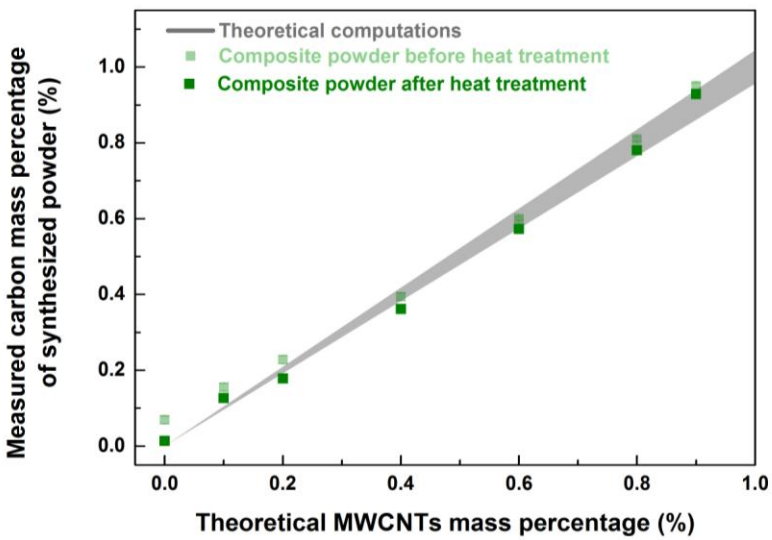

Figure 10 : Comparison of theoretical MWCNTs mass percentage and measured carbon mass percentage of composite powders

First of all, it should be stressed that the experimental values are in line with the theoretical values both before and after the heat treatment. It proves that the estimated concentration of MWCNTs in suspension (C_{MWCNTs}) is close to reality and that the established procedure permits high control of the amount of MWCNTs within the Ag/MWCNTs composite powders. Secondly, the carbon content decreases slightly after the heat treatment which can be due to the decomposition of organic species adsorbed on the surface of Ag particles. The slight decreases also prove that the heat treatment does not induce the decomposition of MWCNTs in the Ag/MWCNTs composite powders as predicted by the thermal analysis. Thus, a heat treatment step can be added to the synthesis protocol of the Ag/MWCNTs composite powder.

Before moving on to the conclusion, it must be emphasized that this non-hazardous synthesis process is very interesting at the industrial scale because it allows to produce easily and at lower cost a large amount of Ag/MWCNTs composite powders with a fraction of individualized MWCNTs compatible with considered application.

3. Conclusion

In summary, Ag/MWCNTs composite powders were successfully synthesized by chemical liquid-phase reduction with mass percentage ranging from 0.1 to 3 wt.%. By controlling the concentration of MWCNTs and keeping the MWCNTs individualized in the

reduction bath, the established procedure lead to the synthesis of Ag/MWCNTs composite powders containing a precise mass percentage of MWCNTs homogeneously dispersed. According to the SEM analysis, MWCNTs are most homogeneously dispersed between 0 to 0.6% by weight of MWCNTs.

Investigations of the reduction of Ag ions by L-AA could be summarized as follow :

1) Concerning synthesis of pure Ag particles, it has been demonstrated by SEM analysis that a temperature increase of 5°C to 70°C and an increase of the excess in L-AA of 1 to 4 accelerates the reduction rate of Ag ions leading to the morphologies of Ag particles switching from compact spherical structures to loose dendritic structures.
2) With high temperature and high amount of L-AA, the addition of the MWCNTs in the reduction bath induces heterogeneous nucleation of Ag particles which increase the nucleation rate of Ag particles. The shape of Ag particles change from dendrites to microscopic spheres to submicron compact spheres respectively with the increase of the concentration of MWCNTs in the reduction bath.
3) As few pollutants are located on the surface of the Ag particles, a heat-treatment has been set up to decompose these pollutants without oxidizing the MWCNTs. The heat treatment must be carried out under Ar gas atmosphere as Ag particles act as catalysts and decrease significantly the oxidation temperature of MWCNTs under ambient air from 600 °C to 350 °C. Quantification of the carbon content of the Ag/MWCNTs composite powders before and after the established heat treatment (350 °C, Ar, 1h) shows no decomposition of the MWCNTs.

The consolidation of these composite powders and the manufacture of Ag/MWCNTs composite materials with high mechanical and thermal properties will be the subject of future studies. Moreover, futures studies could focus on the optimization of the synthesis protocol (nature and amount of surfactant, covalent functionalization of CNTs, complexation of Ag ions, nature of reducing agent …) or on a more thorough characterization of the as-produced Ag/MWCNTs composite powder (characterization of the interfacial crystalline structure, electrocatalytic activity…).

Acknowledgments

The authors would like to thank Eric Lebraud, Dominique Denux and Christine Labrugère of the Institute for Solid State Chemistry of Bordeaux (ICMCB, UMR 5026) for performing the XRD, TGA and XPS analyses, respectively.

References

[1] S. Berber, Y. K. Kwon, and D. Tománek, "Unusually High Thermal Conductivity of Carbon Nanotubes," *Phys. Rev. Lett.*, vol. 84, no. 20, pp. 4613–4616, 2000, doi: 10.1103/PhysRevLett.84.4613.

[2] P. Kim, L. Shi, A. Majumdar, and P. L. McEuen, "Thermal Transport Measurements of Individual Multiwalled Nanotubes," *Phys. Rev. Lett.*, vol. 87, no. 21, p. 215502, 2001, doi: 10.1103/PhysRevLett.87.215502.

[3] M. J. Biercuk, S. Ilani, C. M. Marcus, and P. L. McEuen, "Electrical Transport in Single-Wall Carbon Nanotubes," in *Carbon Nanotubes: Advanced Topics in the Synthesis, Structure, Properties and Applications*, Berlin, Heidelberg: Springer Berlin Heidelberg, 2008, pp. 455–493.

[4] D. J. Yang, Q. Zhang, G. Chen, S. F. Yoon, J. Ahn, S. G. Wang, *et al.*, "Thermal conductivity of multiwalled carbon nanotubes," *Phys. Rev. B*, vol. 66, no. 16, p. 165440, 2002, doi: 10.1103/PhysRevB.66.165440.

[5] M. R. Falvo, G. J. Clary, R. M. Taylor, V. Chi, F. P. Brooks, S. Washburn, *et al.*, "Bending and buckling of carbon nanotubes under large strain," *Nature*, vol. 389, no. 6651, pp. 582–584, 1997, doi: 10.1038/39282.

[6] K. Pietrzak, K. Frydman, D. Wójcik-Grzybek, A. Gładki, A. Bańkowska, and P. Borkowski, "Effect of Carbon Forms on Properties of Ag-C Composites Contact Materials," *Mater. Sci.*, vol. 24, no. 1, pp. 69–74, 2018, doi: 10.5755/j01.ms.24.1.17769.

[7] H. Pal and V. Sharma, "Thermal conductivity of carbon nanotube–silver composite," *Trans. Nonferrous Met. Soc. China*, vol. 25, no. 1, pp. 154–161, 2015, doi: 10.1016/S1003-6326(15)63590-7.

[8] A. Oluwalowo, N. Nguyen, S. Zhang, J. G. Park, and R. Liang, "Electrical and thermal conductivity improvement of carbon nanotube and silver composites," *Carbon*, vol. 146, pp. 224–231, 2019, doi: 10.1016/j.carbon.2019.01.073.

[9] O. K. Abudayyeh, N. D. Gapp, C. Nelson, D. M. Wilt, and S. M. Han, "Silver–Carbon-Nanotube Metal Matrix Composites for Metal Contacts on Space Photovoltaic Cells," *IEEE J. Photovolt.*, vol. 6, no. 1, pp. 337–342, 2016, doi: 10.1109/JPHOTOV.2015.2480224.

[10] S. R. Bakshi, D. Lahiri, and A. Agarwal, "Carbon nanotube reinforced metal matrix composites - a review," *Int. Mater. Rev.*, vol. 55, no. 1, pp. 41–64, 2010, doi: 10.1179/095066009X12572530170543.

[11] J. Hilding, E. A. Grulke, Z. G. Zhang, and F. Lockwood, "Dispersion of Carbon Nanotubes in Liquids," *J. Dispers. Sci. Technol.*, vol. 24, no. 1, pp. 1–41, 2003, doi: 10.1081/DIS-120017941.

[12] M. Pontoreau, E. Le Guen, C. Bourda, and J.-F. Silvain, "Optimization of highly concentrated dispersions of multi-walled carbon nanotubes with emphasis on surfactant content and carbon nanotubes quality," *Nanotechnology*, 2020, doi: 10.1088/1361-6528/ab9d42.

[13] H. K. F. Cheng, Y. Pan, N. G. Sahoo, K. Chong, L. Li, S. Hwa Chan, *et al.*, "Improvement in properties of multiwalled carbon nanotube/polypropylene nanocomposites through homogeneous dispersion with the aid of surfactants," *J. Appl. Polym. Sci.*, vol. 124, no. 2, pp. 1117–1127, 2012, doi: 10.1002/app.35047.

[14] M. S. Strano, V. C. Moore, M. K. Miller, M. J. Allen, E. H. Haroz, C. Kittrell, *et al.*, "The Role of Surfactant Adsoprtion during Ultrasonication in the Dispersion of Single-Walled Carbon Nanotubes," *Journal of Nanoscience and Nanotechnology*, vol. 3, no. 1–2, pp. 81–86, 2003, doi: DOI: info:doi/10.1166/jnn.2003.194.

[15] O. S. Zueva, O. N. Makshakova, B. Z. Idiyatullin, D. A. Faizullin, N. N. Benevolenskaya, A. O. Borovskaya, *et al.*, “Structure and properties of aqueous dispersions of sodium dodecyl sulfate with carbon nanotubes,” *Russ. Chem. Bull.*, vol. 65, no. 5, pp. 1208–1215, 2016, doi: 10.1007/s11172-016-1437-5.

[16] L. Jiang, L. Gao, and J. Sun, “Production of aqueous colloidal dispersions of carbon nanotubes,” *J. Colloid Interface Sci.*, vol. 260, no. 1, pp. 89–94, 2003, doi: 10.1016/S0021-9797(02)00176-5.

[17] J. Rausch, R.-C. Zhuang, and E. Mäder, “Surfactant assisted dispersion of functionalized multi-walled carbon nanotubes in aqueous media,” *Compos. Part Appl. Sci. Manuf.*, vol. 41, no. 9, pp. 1038–1046, 2010, doi: 10.1016/j.compositesa.2010.03.007.

[18] Y. N. Tolchkov, Z. A. Mikhaleva, R. D. A. Sldozian, N. R. Memetov, and A. G. Tkachev, “Effect of Surfactant Stabilizers on the Distribution of Carbon Nanotubes in Aqueous Media,” *J. Wuhan Univ. Technol.-Mater Sci Ed*, vol. 33, no. 3, pp. 533–536, 2018, doi: 10.1007/s11595-018-1855-3.

[19] S. Javadian, A. Motaee, M. Sharifi, H. Aghdastinat, and F. Taghavi, “Dispersion stability of multi-walled carbon nanotubes in catanionic surfactant mixtures,” *Colloids Surf. Physicochem. Eng. Asp.*, vol. 531, pp. 141–149, 2017, doi: 10.1016/j.colsurfa.2017.07.081.

[20] J. Yu, N. Grossiord, C. E. Koning, and J. Loos, “Controlling the dispersion of multi-wall carbon nanotubes in aqueous surfactant solution,” *Carbon*, vol. 45, no. 3, pp. 618–623, 2007, doi: 10.1016/j.carbon.2006.10.010.

[21] P. Yang, X. You, J. Yi, D. Fang, R. Bao, T. Shen, *et al.*, “Simultaneous achievement of high strength, excellent ductility, and good electrical conductivity in carbon nanotube/copper composites,” *J. Alloys Compd.*, vol. 752, pp. 431–439, 2018, doi: 10.1016/j.jallcom.2018.03.341.

[22] J. Li, Y. Li, H. He, and F. Wang, “Preparation and Characterization of solution-processed MWCNT/Ag matrix composite films,” *16th International Conference on Electronic Packaging Technology (ICEPT)*, pp. 1010–1013, 2015.

[23] S. Cho, K. Kikuchi, and A. Kawasaki, “On the role of amorphous intergranular and interfacial layers in the thermal conductivity of a multi-walled carbon nanotube–copper matrix composite,” *Acta Mater.*, vol. 60, no. 2, pp. 726–736, 2012, doi: 10.1016/j.actamat.2011.09.056.

[24] P. Yang, X. You, J. Yi, D. Fang, R. Bao, T. Shen, *et al.*, “Influence of dispersion state of carbon nanotubes on electrical conductivity of copper matrix composites,” *J. Alloys Compd.*, vol. 752, pp. 376–380, 2018, doi: 10.1016/j.jallcom.2018.04.129.

[25] S. Cho, K. Kikuchi, T. Miyazaki, K. Takagi, A. Kawasaki, and T. Tsukada, “Multiwalled carbon nanotubes as a contributing reinforcement phase for the improvement of thermal conductivity in copper matrix composites,” *Scr. Mater.*, vol. 63, no. 4, pp. 375–378, 2010, doi: 10.1016/j.scriptamat.2010.04.024.

[26] L. Jiang, G. Fan, Z. Li, X. Kai, D. Zhang, Z. Chen, *et al.*, “An approach to the uniform dispersion of a high volume fraction of carbon nanotubes in aluminum powder,” *Carbon*, vol. 49, no. 6, pp. 1965–1971, 2011, doi: 10.1016/j.carbon.2011.01.021.

[27] F. Housaer, A. Legris, and F. Beclin, “Elaboration et caractérisation de composites Aluminium/Nanotubes de Carbone obtenus par métallurgie des poudres,” *thesis, Lille 1*, 2015.

[28] A. K. Shukla, N. Nayan, S. V. S. N. Murty, S. C. Sharma, P. Chandran, S. R. Bakshi, *et al.*, “Processing of copper–carbon nanotube composites by vacuum hot pressing technique,” *Mater. Sci. Eng. A*, vol. 560, pp. 365–371, 2013, doi: 10.1016/j.msea.2012.09.080.

[29] K. T. Kim, S. I. Cha, S. H. Hong, and S. H. Hong, “Microstructures and tensile behavior of carbon nanotube reinforced Cu matrix nanocomposites,” *Mater. Sci. Eng. A*, vol. 430, no. 1, pp. 27–33, 2006, doi: 10.1016/j.msea.2006.04.085.
[30] Y. Feng and H. Yuan, “Electroless plating of carbon nanotubes with silver,” *J. Mater. Sci.*, vol. 39, no. 9, pp. 3241–3243, 2004, doi: 10.1023/B:JMSC.0000025869.05546.94.
[31] S. Arai and J. Fujii, “Electroless Deposition of Silver on Multiwalled Carbon Nanotubes Using Iodide Bath,” *J. Electrochem. Soc.*, vol. 158, no. 8, p. D506, 2011, doi: 10.1149/1.3599066.
[32] M. Lis, A. Wrona, J. Mazur, C. Dupont, M. Kamińska, D. Kopyto, *et al.*, “Fabrication And Properties Of Silver Based Multiwall Carbon Nanotube Composite Prepared By Spark Plasma Sintering Method,” *Arch. Metall. Mater.*, vol. 60, no. 2, pp. 1351–1355, 2015, doi: 10.1515/amm-2015-0129.
[33] Y. X. You, Y. Ye, Y. J. Su, Q. Z. Tang, and T. L. Guo, “Preparation and Field Emission Properties of Ag-CNTs by Electroless Plating,” *Adv. Mater. Res.*, vol. 148–149, pp. 983–986, 2010, doi: 10.4028/www.scientific.net/AMR.148-149.983.
[34] C. S. Wu, C. Y. Lee, J. K. Chen, S. W. Kuo, S. K. Fan, C.-C. Cheng, *et al.*, “Microwave-assisted Electroless Deposition of Silver Nanoparticles onto Multiwalled Carbon Nanotubes,” *Int J Electrochem Sci*, vol. 7, p. 10, 2012.
[35] Q. Zhao, M. Xie, Y. Liu, and J. Yi, “Improved electroless plating method through ultrasonic spray atomization for depositing silver nanoparticles on multi-walled carbon nanotubes,” *Appl. Surf. Sci.*, vol. 409, no. Supplement C, pp. 164–168, 2017, doi: 10.1016/j.apsusc.2017.03.032.
[36] W. M. Daoush, B. K. Lim, D. H. Nam, and S. H. Hong, “Microstructure and mechanical properties of CNT/Ag nanocomposites fabricated by spark plasma sintering,” *J. Exp. Nanosci.*, vol. 9, no. 6, pp. 588–596, 2014, doi: 10.1080/17458080.2012.680927.
[37] Q. Zhao, S. Tan, M. Xie, Y. Liu, and J. Yi, “A study on the CNTs-Ag composites prepared based on spark plasma sintering and improved electroless plating assisted by ultrasonic spray atomization,” *J. Alloys Compd.*, vol. 737, pp. 31–38, 2018, doi: 10.1016/j.jallcom.2017.12.066.
[38] K. S. Kim, B. G. Park, H. Kim, H. S. Lee, and S. B. Jung, “Fabrication of Ag-MWNT nanocomposite paste for high-power LED package,” *Curr. Appl. Phys.*, vol. 15, pp. S36–S41, 2015, doi: 10.1016/j.cap.2015.03.006.
[39] H. Pal, V. Sharma, R. Kumar, and N. Thakur, “Facile Synthesis and Electrical Conductivity of Carbon Nanotube Reinforced Nanosilver Composite,” *Z. Für Naturforschung A*, vol. 67, no. 12, pp. 679–684, 2012, doi: 10.5560/zna.2012-0072.
[40] H. Pal, V. Sharma, and M. Sharma, “Influence of functionalization on mechanical and electrical properties of carbon nanotube-based silver composites,” *Philos. Mag.*, vol. 94, no. 13, pp. 1478–1492, 2014, doi: 10.1080/14786435.2014.892221.
[41] S. I. Cha, K. T. Kim, S. N. Arshad, C. B. Mo, and S. H. Hong, “Extraordinary Strengthening Effect of Carbon Nanotubes in Metal-Matrix Nanocomposites Processed by Molecular-Level Mixing,” *Adv. Mater.*, vol. 17, no. 11, pp. 1377–1381, 2005, doi: 10.1002/adma.200401933.
[42] K. T. Kim, S. I. Cha, and S. H. Hong, “Hardness and wear resistance of carbon nanotube reinforced Cu matrix nanocomposites,” *Mater. Sci. Eng. A*, vol. 449–451, pp. 46–50, 2007, doi: 10.1016/j.msea.2006.02.310.
[43] H. Pal and V. Sharma, “Effect of sintering on mechanical and electrical properties of carbon nanotube based silver nanocomposites,” *Indian J. Phys.*, vol. 89, no. 3, pp. 217–224, 2015, doi: 10.1007/s12648-014-0539-x.

[44] S. Wu and S. Meng, “Preparation of ultrafine silver powder using ascorbic acid as reducing agent and its application in MLCI,” *Mater. Chem. Phys.*, vol. 89, no. 2, pp. 423–427, 2005, doi: 10.1016/j.matchemphys.2004.09.026.
[45] S. Gu, W. Wang, H. Wang, F. Tan, X. Qiao, and J. Chen, “Effect of aqueous ammonia addition on the morphology and size of silver particles reduced by ascorbic acid,” *Powder Technol.*, vol. 233, pp. 91–95, 2013, doi: 10.1016/j.powtec.2012.08.036.
[46] G. Guo, W. Gan, J. Luo, F. Xiang, J. Zhang, H. Zhou, *et al.*, “Preparation and dispersive mechanism of highly dispersive ultrafine silver powder,” *Appl. Surf. Sci.*, vol. 256, no. 22, pp. 6683–6687, 2010, doi: 10.1016/j.apsusc.2010.04.070.
[47] J. Liu, T. Yang, C. Li, J. Dai, and Y. Han, “Reversibly Switching Silver Hierarchical Structures via Reaction Kinetics,” *Sci. Rep.*, vol. 5, no. 1, pp. 1–8, 2015, doi: 10.1038/srep14942.
[48] T. A. Witten and L. M. Sander, “Diffusion-Limited Aggregation, a Kinetic Critical Phenomenon,” *Phys. Rev. Lett.*, vol. 47, no. 19, pp. 1400–1403, 1981, doi: 10.1103/PhysRevLett.47.1400.
[49] G. Zhang, S. Sun, M. N. Banis, R. Li, M. Cai, and X. Sun, “Morphology-Controlled Green Synthesis of Single Crystalline Silver Dendrites, Dendritic Flowers, and Rods, and Their Growth Mechanism,” *Cryst. Growth Des.*, vol. 11, no. 6, pp. 2493–2499, 2011, doi: 10.1021/cg200256j.
[50] J. Fang, H. You, P. Kong, Y. Yi, X. Song, and B. Ding, “Dendritic Silver Nanostructure Growth and Evolution in Replacement Reaction,” *Cryst. Growth Des.*, vol. 7, no. 5, pp. 864–867, 2007, doi: 10.1021/cg0604879.
[51] V. Georgakilas, D. Gournis, V. Tzitzios, L. Pasquato, D. M. Guldi, and M. Prato, “Decorating carbon nanotubes with metal or semiconductor nanoparticles,” *J. Mater. Chem.*, vol. 17, no. 26, pp. 2679–2694, 2007, doi: 10.1039/B700857K.
[52] Y. Wang, X. Xu, Z. Tian, Y. Zong, H. Cheng, and C. Lin, “Selective Heterogeneous Nucleation and Growth of Size-Controlled Metal Nanoparticles on Carbon Nanotubes in Solution,” *Chem. – Eur. J.*, vol. 12, no. 9, pp. 2542–2549, 2006, doi: 10.1002/chem.200501010.
[53] Z. Tan, H. Abe, M. Naito, and S. Ohara, “Arrangement of palladium nanoparticles templated by supramolecular self-assembly of SDS wrapped on single-walled carbon nanotubes,” *Chem. Commun.*, vol. 46, no. 24, pp. 4363–4365, 2010, doi: 10.1039/C0CC00099J.
[54] S. Al Aani, V. Gomez, C. J. Wright, and N. Hilal, “Fabrication of antibacterial mixed matrix nanocomposite membranes using hybrid nanostructure of silver coated multi-walled carbon nanotubes,” *Chem. Eng. J.*, vol. 326, pp. 721–736, 2017, doi: 10.1016/j.cej.2017.06.029.